Reactivity of Tetraneopentylhafnium, $Hf(CH_2tBu)_4$, with Silica Surfaces

Géraldine Tosin, Catherine C. Santini,* Mostafa Taoufik, Aimery De Mallmann, and Jean-Marie Basset

Laboratoire de Chimie OrganoMétallique de surface (LCOMS), UMR 9986 CNRS, ESCPE Lyon, 43, boulevard du 11 novembre 1918, 69616 Villeurbanne Cedex, France

Received February 23, 2006

The reaction of $Hf(CH_2tBu)_4$ with a silica surface treated at 800 °C affords a unique surface organometallic species in only one surface environment, $(\equiv SiO)Hf(CH_2tBu)_3$ (**1**-$SiO_{2-(800)}$). In contrast, with $SiO_{2-(500)}$ two surface species, $(\equiv SiO)Hf(CH_2tBu)_3$ (**1**-$SiO_{2-(500)}$) and $(\equiv SiO)_2Hf(CH_2tBu)_2$ (**2**−$SiO_{2-(500)}$), in a molar ratio of 70:30 are obtained. Thermal treatment of **1**-$SiO_{2-(800)}$ at increasing temperatures leads to the successive evolution of neopentane, isobutene, and isobutane as well as several alkanes varying from C_1 to C_5. Polyisobutenes are also formed on the surface. The mechanism by which such decomposition occurs suggests a succession of γ-H eliminations with formation of neopentane followed by β-methyl transfer and formation of isobutene and [Hf]−Me. This isobutene is reinserted into [Hf]−Me with formation of isopentene and [Hf]−H. A comparison of the analytical data of **1**-$SiO_{2-(800)}$ and $(\equiv SiO)Zr(CH_2tBu)_3$ indicated the hafnium complex exhibits in EXAFS shorter Hf−C and Hf−O bonds and a larger Hf−C_α−C_β angle and in 2D *J*-resolved NMR spectra a lower $^1J(C_\alpha-H)$ value. These differences underlined a larger steric hindrance in the coordination sphere of the Hf metal. The thermal stability of **1**-$SiO_{2-(800)}$ was monitored by infrared spectroscopy, in batch and continuous flow reactors, and proved that **1**-$SiO_{2-(800)}$ was more stable than $(\equiv SiO)Zr(CH_2tBu)_3$ and more active in alkane hydrogenolysis.

Introduction

Surface organometallic chemistry represents an approach to the preparation of well-defined active sites, the possibility of observing elementary reaction steps, and the development of a fundamental basis for the synthesis of tailor-made catalysts.[1]

Access to a single site is the main objective of this approach. The first step for the synthesis of tailor-made catalysts, developed in our laboratory,[1−5] consists of the reaction of alkyl complexes MR_n with surface oxide. In the case of silica treated at temperatures above 500 °C, the major pathway is the protolysis of one of the M−C bonds by one surface silanol (≡Si−OH) to form a ≡SiO−M bond. In this way, well-defined monosiloxy surface complexes are obtained, such as $[(\equiv SiO)Zr(CH_2tBu)_3]$,[2−4] $[(\equiv SiO)Ta(=CHtBu)(CH_2tBu)_2]$, $[(\equiv SiO)TaCp^*(Me)_3]$, and $[(\equiv SiO)W(\equiv CtBu)(CH_2tBu)_2]$.[5]

Surface complexes of group 4, $(\equiv SiO)M(CH_2tBu)_3$ (M = Ti, Zr), are precursors to several relatively well-defined active heterogeneous catalysts. $(\equiv SiO)Zr(CH_2tBu)_3$ under dihydrogen generates a mixture of $(\equiv SiO)_3ZrH$ and $(\equiv SiO)_2ZrH_2$,[6] active in Ziegler−Natta polymerization,[7−9] hydrogenolysis of polyethylene and polypropylene,[10] alkane hydrogenolysis,[2] and hydrogenation.[7−9,11] $(\equiv SiO)Ti(CH_2tBu)_3$ under dihydrogen generates $(\equiv SiO)_3TiH$, which is active in hydrogenolysis, isomerization of light alkanes,[12] and epoxidation of 1-octene in the presence of a *t*BuOH/*t*BuOOH mixture.[13]

In contrast, data on the characterization and catalytic properties of hafnium surface complexes are very scarce.[14,15] However, in some papers the hafnium complexes are described in comparison to the zirconium analogue as being more active in the polymerization of ethylene,[16] more selective in the oligomerization of propene,[17,18] and faster in the hydrogenolysis of butane.[19] These differences in the activity could be related to

* To whom correspondence should be addressed. Fax: 04 72 43 17 95. E-mail: santini@cpe.fr.

(1) Coperet, C.; Chabanas, M.; Saint-Arroman, R. P.; Basset, J.-M. *Angew. Chem., Int. Ed.* **2003**, *42*, 156−181.
(2) Quignard, F.; Choplin, A.; Basset, J. M. *Chem. Commun.* **1991**, 1589−1590.
(3) Lecuyer, C.; Quignard, F.; Choplin, A.; Olivier, D.; Basset, J. M. *Angew. Chem., Int. Ed. Engl.* **1991**, *30*, 1660−1661.
(4) Corker, J.; Lefebvre, F.; Lecuyer, C.; Dufaud, V.; Quignard, F.; Choplin, A.; Evans, J.; Basset, J.-M. *Science* **1996**, *271*, 966−969.
(5) Le Roux, E.; Taoufik, M.; Chabanas, M.; Alcor, D.; Baudouin, A.; Coperet, C.; Thivolle-Cazat, J.; Basset, J.-M.; Lesage, A.; Hediger, S.; Emsley, L. *Organometallics* **2005**, *24*, 4274−4279.
(6) Rataboul, F.; Baudouin, A.; Thieuleux, C.; Veyre, L.; Coperet, C.; Thivolle-Cazat, J.; Basset, J.-M.; Lesage, A.; Emsley, L. *J. Am. Chem. Soc.* **2004**, *126*, 12541−12550.
(7) Zakharov, V. A.; Dudchenko, V. K.; Paukstis, E.; Karakchiev, L. G.; Ermakov, Y. I. *J. Mol. Catal.* **1977**, *2*, 421−435.
(8) Zakharov, V. A.; Yermakov, Y. I. *Catal. Rev.* **1979**, *19*, 67−103.
(9) Zakharov, V. A.; Ryndin, Y. A. *J. Mol. Catal.* **1989**, *56*, 183−193.
(10) Dufaud, V.; Basset, J.-M. *Angew. Chem., Int. Ed.* **1998**, *37*, 806−810.
(11) Schwartz, J.; Ward, M. D. *J. Mol. Catal.* **1980**, *8*, 465−469.
(12) Rosier, C.; Niccolai, G. P.; Basset, J.-M. *J. Am. Chem. Soc.* **1997**, *119*, 12408−12409.
(13) Rosier, C.; Bini, F.; Saint-Arroman, R. P.; Neumann, E.; Dablemont, C.; de Mallmann, A.; Niccolai, G. P.; Lefebvre, F.; Basset, J. M.; Crocker, M.; Buijink, J.-K. Submitted for publication in *Organometallics*.
(14) Saint-Arroman, R. P.; Basset, J.-M.; Lefebvre, F.; Didillon, B. *Appl. Catal. A* **2005**, *290*, 181−190.
(15) d'Ornelas, L.; Reyes, S.; Quignard, F.; Choplin, A.; Basset, J. M. *Chem. Lett.* **1993**, 1931−1934.
(16) Schock, L. E.; Marks, T. J. *J. Am. Chem. Soc.* **1988**, *110*, 7701−7715.
(17) Eshuis, J. J. W.; Tan, Y. Y.; Teuben, J. H.; Renkema, J. *J. Mol. Catal.* **1990**, *62*, 277−287.
(18) Eshuis, J. J. W.; Tan, Y. Y.; Meetsma, A.; Teuben, J. H.; Renkema, J.; Evens, G. G. *Organometallics* **1992**, *11*, 362−369.
(19) Basset, J.-M.; Niccolai, G. P. *Surface Organometallic Chemistry*; Wiley: Weinheim, Germany, 2002; Vol. 2.

10.1021/om060178f CCC: $33.50
Publication on Web 06/01/2006

the higher stability of the Hf−C bond (D_{Zr-C} = 54 kcal/mol, D_{Hf-C} = 58 kcal/mol),[20] which induces a more stable catalyst. A further tendency to undergo β-methyl transfer,[16,21,22] due to a higher steric hindrance in the coordination sphere of Hf compared to that of Zr, has also been reported.[23] Moreover, as the Hf−O bond is more stable than the Zr−O bond, the risk of metal leaching could be reduced.[24]

Therefore, Hf complexes seem to be good candidates in several catalytic reactions. However, information and data are needed to develop the use of hafnium surface complexes in catalysis. We report in this paper the reaction of Hf(CH$_2$*t*Bu)$_4$ with silica surfaces dehydroxylated at 800 and 500 °C and compare the results with those for zirconium analogues.

Results and Discussion

Flame Aerosil silica from Degussa was dehydroxylated at 800 °C ($SiO_{2-(800)}$) and at 500 °C ($SiO_{2-(500)}$). The specific surface areas are 180 and 200 m^2 g^{-1}, respectively, and the amounts of silanol groups, determined by quantitative solid-state ^{1}H NMR and by reaction with CH_3Li, are 0.6 ± 0.1 and 1.4 ± 0.1 OH nm^{-2}, respectively. The high dehydroxylation temperature causes the condensation of isolated hydroxyl groups, giving rise to highly strained and reactive (≡Si−O−Si≡) bridges with a density of 0.1 (≡Si−O−Si≡) nm^{-2} at 800 °C.[25,26]

The usual synthesis of Hf(CH$_2$*t*Bu)$_4$ is carried out by the reverse addition of $HfCl_4$ (4 mmol) into a solution of *t*BuCH$_2$-Li.[27,28] The white crystalline solid, purified by sublimation (70 °C, 10^{-5} mbar), is obtained in 15% yield from *t*BuCH$_2$Cl.

To increase this yield, in particular when labeled *t*Bu^{13}CH$_2$-Cl is used as the starting material, the preparation has been reinvestigated.[28,29] The Grignard reagent *t*BuCH$_2$MgCl or *t*Bu^{13}-CH$_2$MgCl in diethyl ether/THF was added to a solution of $HfCl_4$ in diethyl ether at 25 °C. Filtration, extraction in pentane, and sublimation (70 °C, 10^{-5} Torr) led to Hf(CH$_2$*t*Bu)$_4$ in 45% yield instead of 15% yield from *t*BuCH$_2$Cl. Zr(CH$_2$*t*Bu)$_4$ and Zr(^{13}-CH$_2$*t*Bu)$_4$ were prepared as already reported.[27]

Reactivity of M(CH$_2$*t*Bu)$_4$ (M = Zr, Hf) with Silica Dehydroxylated at 800 °C ($SiO_{2-(800)}$). Two different workups were used in order to graft Hf(CH$_2$*t*Bu)$_4$ onto $SiO_{2-(800)}$: either impregnation in a solvent (pentane) at room temperature or mechanical mixing at 70 °C, in each case for 2 h. In the case of impregnation, the elimination of the excess complex was completed by washing the solid several times with the same solvent (filtration/distillation cycles). In the case of the mechanical mixture, pentane was introduced at the end of the reaction after cooling, and then the solid was washed using the same procedure as above. In both cases the product formed was the same, and the percentage of hafnium grafted was similar. A typical procedure using the impregnation method is described below.

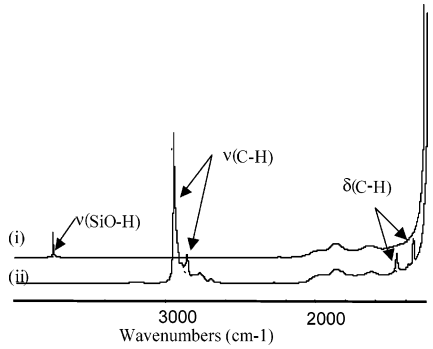

Figure 1. IR spectra: (i) $SiO_{2-(800)}$; (ii) sample after sublimation of Hf(CH$_2$*t*Bu)$_4$ followed by vacuum treatment (10^{-5} Torr) at 70 °C for 1 h.

The reaction of Hf(CH$_2$*t*Bu)$_4$ with $SiO_{2-(800)}$ was achieved by stirring for 2 h at 25 °C a mixture of 166 mg of Hf(CH$_2$*t*Bu)$_4$ (360 μmol) with 1.43 g of silica (256 μmol (≡SiOH)) in pentane. The evolution of 300 μmol of neopentane as the only gaseous product was detected by gas chromatography. This corresponds to 0.9 ± 0.1 neopentane formed per initial available surface (≡SiOH). The resulting white surface organometallic species Hf(CH$_2$*t*Bu)$_4$/$SiO_{2-(800)}$, obtained after washing the excess of Hf(CH$_2$*t*Bu)$_4$ and drying under high vacuum at 25 °C, contains 3.5 wt % of Hf (0.66 Hf/nm^2). This corresponds to 1.1 ± 0.1 Hf per initial surface (≡SiOH). Elemental analyses indicate the presence of 14 ± 2 C per grafted Hf atom (3.5 ± 0.2 wt % Hf, 3.2 ± 0.2 wt % C). The hydrolysis of Hf(CH$_2$*t*Bu)$_4$/$SiO_{2-(800)}$ at 25 °C produced 2.5 ± 0.2 equiv of neopentane per Hf. Finally hydrogenolysis of the species at 150 °C for 17 h led to the formation of methane (9 mol) and of ethane (3 mol) per mol of grafted hafnium: i.e., 15 ± 2 C per Hf grafted.

The reaction of Zr(CH$_2$*t*Bu)$_4$ with $SiO_{2-(800)}$ was achieved under the same experimental conditions as for Hf(CH$_2$*t*Bu)$_4$, using the impregnation workup (73 mg of Zr(CH$_2$*t*Bu)$_4$ (190 μmol) and 0.9 g of silica (160 μmol (≡SiOH))). The results of elemental analyses and quantification of the gas evolved during the grafting and the hydrogenolysis were very similar to those observed for Hf compounds.

The results of infrared spectroscopy are represented in Figure 1. Upon grafting, there was total disappearance of the ν(O−H) band at 3747 cm^{-1} attributed to isolated silanol groups and the concomitant emergence of bands at 2955 (ν_{as}(CH$_3$)), 2867 (ν_s-(CH$_3$)), 1466 (δ_{as}(CH$_3$)), and 1364 cm^{-1} (δ_s(CH$_3$)) characteristic of the neopentyl ligands. Sublimation of Zr(CH$_2$*t*Bu)$_4$ onto $SiO_{2-(500)}$ lead to the appearance of the same bands.[30]

The ^{1}H MAS NMR spectrum of Hf(CH$_2$*t*Bu)$_4$/$SiO_{2-(800)}$ (Figure 2i) shows one peak at 0.8 ppm attributed to the protons of the methyl groups of Hf(CH$_2$C(C*H*$_3$)$_3$) similar to the resonance at 0.7 ppm observed in the case of (≡SiO)Zr-(CH$_2$*t*Bu)$_3$.[14,15] Note that the peak due to free silanols at 1.8 ppm is absent in the two spectra, confirming their total consumption, as already suggested by IR data.

The solid-state ^{13}C CP-MAS NMR spectrum of Hf(CH$_2$*t*Bu)$_4$/$SiO_{2-(800)}$ (Figure 2ii) exhibits two different peaks at 34 and 106 ppm. The former is assigned to the methyl groups of the neopentyl moieties Hf(CH$_2$C(*C*H$_3$)$_3$), while the latter corresponds probably to the secondary carbon of the ligand, Hf-

(20) Davidson, P. J.; Lappert, M. F.; Pearce, R. *Chem. Rev.* **1976**, *76*, 219−242.
(21) Lappert, M. F.; Patil, D. S.; Pedley, J. B. *Chem. Commun.* **1975**, 830−831.
(22) Wu, Y.-D.; Peng, Z.-H.; Chan, K. W. K.; Liu, X.; Tuinman, A. A.; Xue, Z. *Organometallics* **1999**, *18*, 2081−2090.
(23) Beswick, C. L.; Marks, T. J. *J. Am. Chem. Soc.* **2000**, *122*, 10358−10370.
(24) Cardin, D. J.; Lappert, M. F.; Raston, C. L. *Chemistry of Organo-Zirconium and Organo-Hafnium Compounds*; Wiley: New York, 1986.
(25) Millot, N.; Santini, C. C.; Lefebvre, F.; Basset, J.-M. *C. R. Chim.* **2004**, *7*, 725−736.
(26) Millot, N.; Soignier, S.; Santini, C. C.; Baudouin, A.; Basset, J.-M. Submitted for publication.
(27) Davidson, P. J.; Lappert, M. F.; Pearce, R. *J. Organomet. Chem.* **1973**, *57*, 269−277.
(28) Schrock, R. R.; Fellmann, J. D. *J. Am. Chem. Soc.* **1978**, *100*, 3359−3370.
(29) Ahn, H.; Marks, T. J. *J. Am. Chem. Soc.* **2002**, *124*, 7103−7110.
(30) Quignard, F.; Lecuyer, C.; Bougault, C.; Lefebvre, F.; Choplin, A.; Olivier, D.; Basset, J. M. *Inorg. Chem.* **1992**, *31*, 928−930.

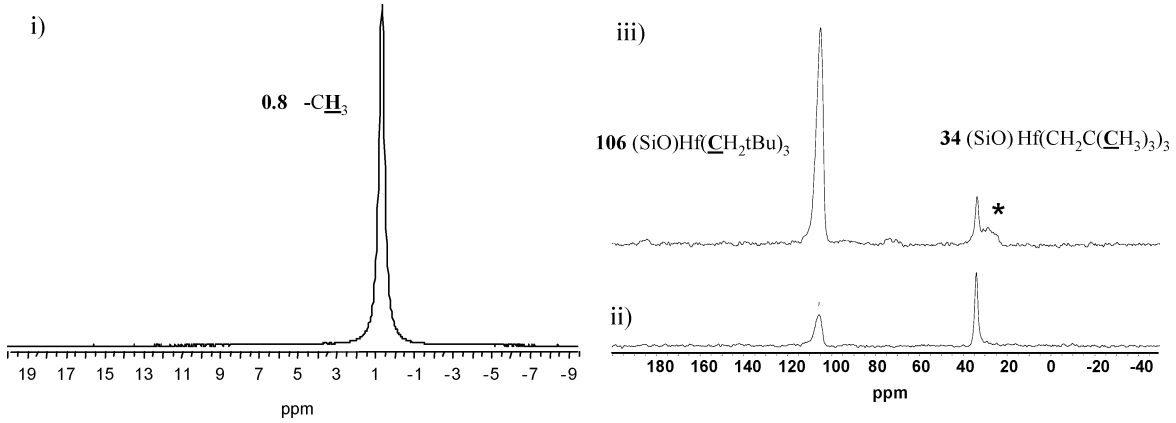

Figure 2. NMR spectra of (≡SiO)Hf(CH_2tBu)$_3$: (i) ^{1}H MAS; (ii) ^{13}C CP-MAS; (iii) ^{13}C CP-MAS of ^{13}C-labeled compound (the asterisk indicates an impurity).

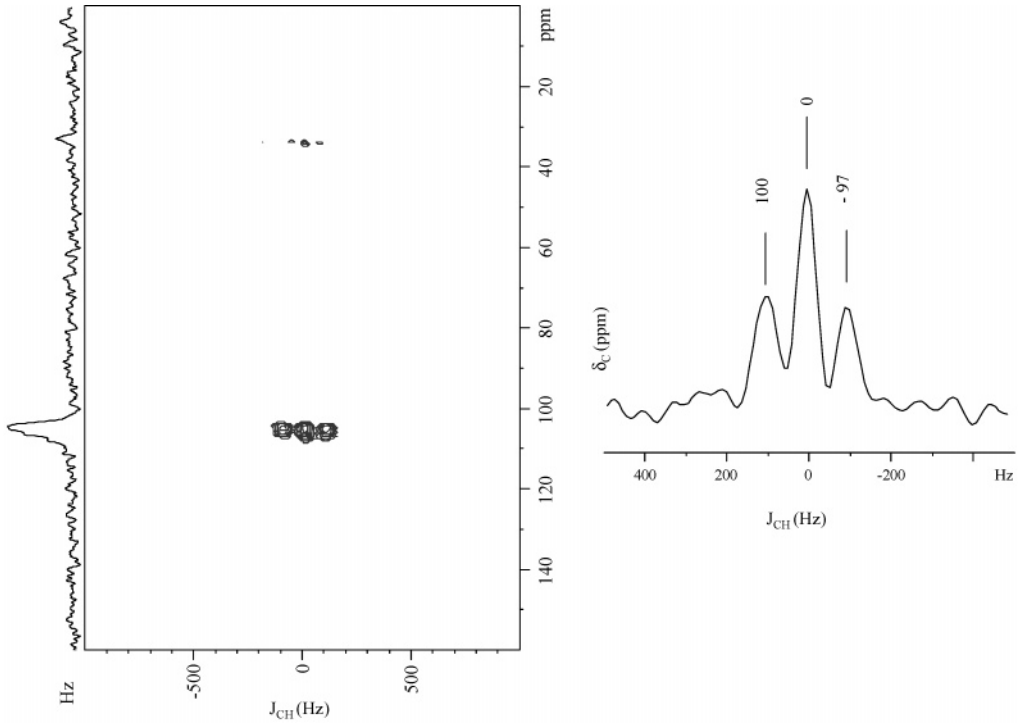

Figure 3. 2D *J*-resolved solid-state NMR spectrum of Hf($^{13}CH_2tBu$)$_4$/$SiO_{2-(800)}$ (left) and trace extracted along the ω_1 dimension of the 2D *J*-resolved spectrum at δ 106 ppm (right).

($CH_2C(CH_3)_3$). The ^{13}C-labeled surface species Hf($^{13}CH_2tBu$)$_4$/$SiO_{2-(800)}$, resulting from the reaction of Hf($^{13}CH_2tBu$)$_4$ with $SiO_{2-(800)}$ (Figure 2iii), exhibits a very intense signal at 106 ppm, confirming these attributions. No resonance for the quaternary carbon, Hf($CH_2C(CH_3)_3$), is observed. The solid-state ^{13}C CP-MAS NMR spectrum Zr(CH_2tBu)$_4$/$SiO_{2-(800)}$ exhibits two different peaks at 33 and 93 ppm attributed to Zr($CH_2C(CH_3)_3$) and Zr($CH_2C(CH_3)_3$), respectively, according to the literature.[14]

It is worth noting that the chemical shifts of zirconium derivatives in ^{13}C NMR (solution or solid state) are always upfield compared to those of the hafnium homologues, $\delta(C_\alpha\text{-(Zr)}) < \delta(C_\alpha\text{(Hf)})$.

2D *J*-resolved NMR spectroscopy is the technique of choice to assign the multiplicity of carbons and to determine in particular $^1J(C_\alpha-H)$ of the **CH**$_2$ in the neopentyl ligand. For Hf(CH_2tBu)$_4$/$SiO_{2-(800)}$ the peak at 106 ppm appears as a triplet with $^1J(C_\alpha-H) = 100 \pm 5$ Hz, (Figure 3) while the $^1J(C_\alpha-H)$ value was 110 ± 5 Hz for Zr(CH_2tBu)$_4$/$SiO_{2-(800)}$ (Figure 4). The slightly smaller $^1J(C_\alpha-H)$ value for the Hf complex might be correlated to its more electrophilic character.[24] At this point, the analytical data did not reveal the presence of a weak agnostic interaction of $C_\alpha-H$ with the metal center.

The surface species Hf(CH_2tBu)$_4$/$SiO_{2-(800)}$ was studied by EXAFS spectroscopy. Figure 5 shows the experimental and fitted EXAFS signals. The fit corresponds to a first coordination sphere of ca. one oxygen atom at 1.95 Å and three carbon atoms at 2.19 Å coordinated to hafnium, which can be respectively assigned to a σ-bonded siloxy ($-O$Si≡) and to the three σ-bonded carbons of the neopentyl groups ($-CH_2tBu$). The Hf−O bond length is similar to the values obtained from X-ray crystallographic studies for hafnium complexes containing silsesquioxane either siloxy or hydroxy groups: i.e. Cp_2Hf(c-$C_5H_9)_7Si_7O_{11}$(OSiMe_2R) (1.97 Å), ^{31}Hf[OSi(O*t*Bu)$_3$]$_4$ and Hf-[OSi(O*t*Bu)$_3$]$_4$(H_2O) (1.912−1.929 Å),[32,33] and Hf(OH)$_4$ (1.939

(31) Wada, K.; Itayama, N.; Watanabe, N.; Bundo, M.; Kondo, T.; Mitsudo, T. *Organometallics* **2004**, *23*, 5824−5832.
(32) Terry, K. W.; Lugmair, C. G.; Tilley, T. D. *J. Am. Chem. Soc.* **1997**, *119*, 9745−9756.
(33) Lugmair, C. G.; Tilley, T. D. *Inorg. Chem.* **1998**, *37*, 764−769.

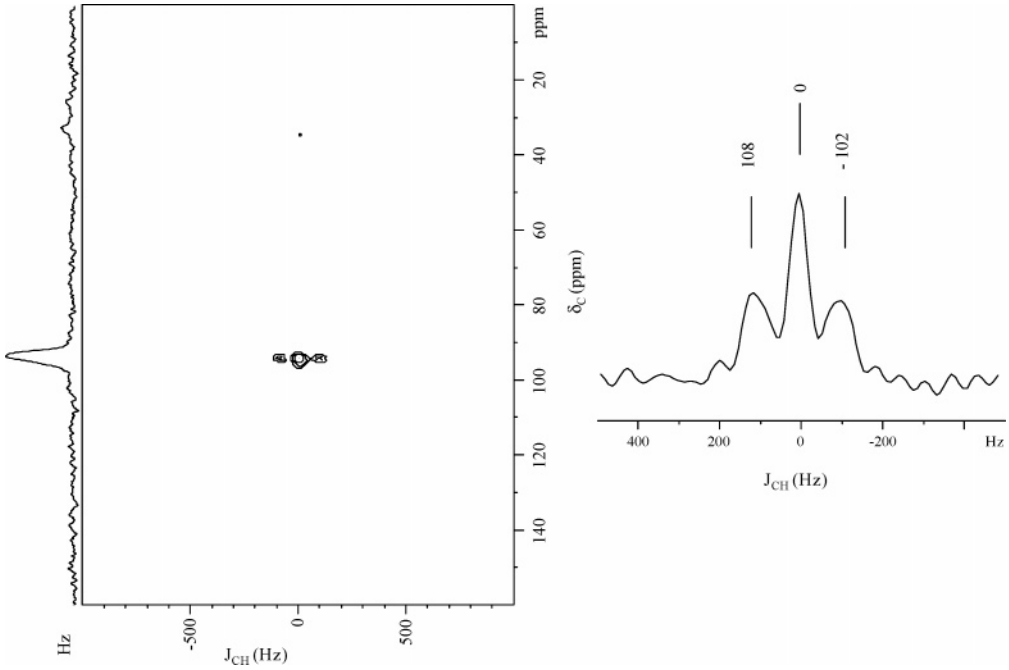

Figure 4. 2D *J*-resolved solid-state NMR spectrum of Zr(^{13}CH$_2$*t*Bu)$_4$/SiO$_{2-(800)}$ (left) and trace extracted along the ω_1 dimension of the 2D *J*-resolved spectrum at δ 93 ppm (right).

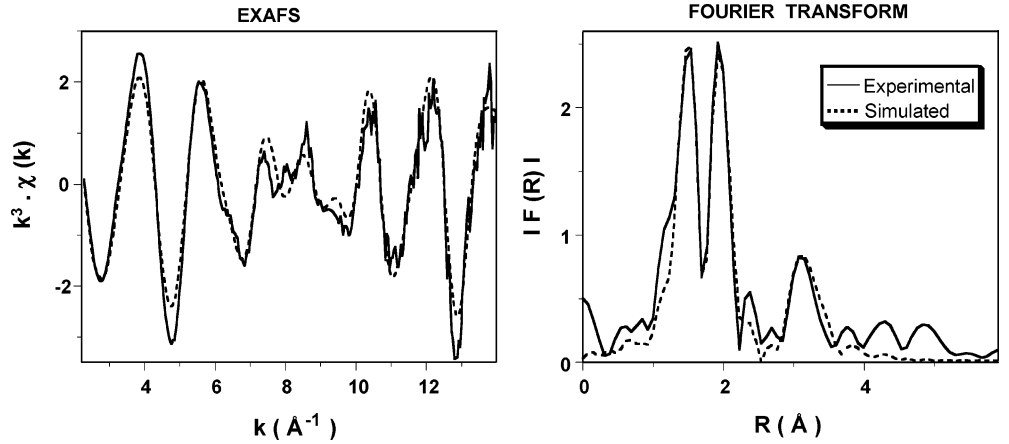

Figure 5. Hf L$_{III}$-edge-weighted EXAFS (left) and corresponding Fourier transform (right) for the solid Hf(CH$_2$*t*Bu)$_4$/SiO$_{2-(800)}$ and comparison to simulation curves: (solid lines) experimental data; (dashed lines) spherical wave theory.

Å).[34] The Hf−C distance (2.191(7) Å) is very similar to one that we found by EXAFS for Hf(CH$_2$*t*Bu)$_4$ in benzene (2.19(1) Å), our reference sample. This distance is also consistent with, though slightly shorter than, the corresponding bond distances reported for analogous molecular complexes, such as Cp*Hf(Me)$_2$[N(Et)C(Me)N(*t*Bu)] (2.247 and 2.253 Å),[35] [MesNON]Hf(CH$_2$*t*Bu)$_2$ (2.210 and 2.225 Å),[36] [Cp*Hf(CH$_2$CHMe$_2$)THF]$^+$ (2.241 Å),[37] [Ar$_{Cl}$N$_2$NMe]Hf(*i*Bu)$_2$ (2.22 Å),[38] and [P$_2$N$_2$]HfMe$_2$ (2.263 and 2.277 Å).[39]

Two additional shells could be added to improve the fit, one including ca. three nonbonding carbons at 3.49(3) Å, corresponding to the quaternary carbon atoms of the neopentyl ligands, and the other ca. one silicon at 3.53(3) Å, corresponding to the silicon atom of a ≡SiO−Hf moiety. The EXAFS-derived parameters are collected in Table 1. With a k^1 weighting the results of the fit were very similar.

Table 1. Hf L$_{III}$-Edge EXAFS-Derived Structural Parameters (k^3 Weighting) for Hf(CH$_2$*t*Bu)$_4$/SiO$_{2-(800)}$[a]

scatterer	coord no.	dist from Hf (Å)	Debye−Waller factor (σ^2/Å^2)
−*O*Si≡	1.1(3)	1.947(7)	0.0009(6)
−*C*H$_2$CMe$_3$	2.9[b]	2.191(7)	0.0027(7)
−CH$_2$*C*′Me$_3$	2.9[b]	3.49(3)	0.002(6)
−O*Si*≡	1.1[b]	3.53(3)	0.002[b]

[a] The values given in parentheses represent the statistical errors generated in the "RoundMidnight" EXAFS fitting program. Conditions: fit range, $\Delta k = 2.3-14.0$ Å^{-1}, $\Delta R = 0.7-3.7$ Å; fit residue, $\rho = 7.8\%$; overall scale factor, $S_0^2 = 0.95$; energy shift, $\Delta E_0 = 4.7(8)$ eV, the same for all shells; number of parameters fitted, $P = 9$; number of degrees of freedom in the fit, $\nu = 13$; quality factor of the fit, $(\Delta\chi)^2/\nu = 1.45$. [b] Shell constrained to the parameter above: $N_O + N_C = 4.0$; $N_{C'} = N_C$; $N_{Si} = N_O$; $\sigma_{Si} = \sigma_{C'}$.

The comparison of these results with the EXAFS-derived parameters obtained for (≡SiO)Zr(CH$_2$*t*Bu)$_3$ grafted onto

(34) Wang, X.; Andrews, L. *Inorg. Chem.* **2005**, *44*, 7189−7193.
(35) Kissounko, D. A.; Zhang, Y.; Harney, M. B.; Sita, L. R. *Adv. Synth. Catal.* **2005**, *347*, 426−432.
(36) Liang, L.-C.; Schrock, R. R.; Davis, W. M. *Organometallics* **2000**, *19*, 2526−2531.
(37) Guo, Z.; Swenson, D. C.; Jordan, R. F. *Organometallics* **1994**, *13*, 1424−1432.
(38) Schrock, R. R.; Adamchuk, J.; Ruhland, K.; Lopez, L. P. H. *Organometallics* **2005**, *24*, 857−866.
(39) Fryzuk, M. D.; Corkin, J. R.; Patrick, B. O. *Can. J. Chem.* **2003**, *81*, 1376−1387.

Table 2. Analytical Data of the Grafting of $Hf(CH_2tBu)_4$ onto $SiO_{2-(500)}$[a]

≡SiOH, nm^{-2}	Hf, nm^{-2}	Hf/(≡SiOH)	wt % Hf	wt % C	C/Hf	CH_3tBu/Hf grafting	CH_3tBu/≡SiOH grafting	CH_3tBu/Hf hydrogenolysis
1.4 ± 0.1	0.8 ± 0.1	0.6 ± 0.1	5.0 ± 0.2	4.1 ± 0.2	12 ± 2	1.3 ± 0.1	0.8 ± 0.1	2.8 ± 0.2 (8.5 CH_4 + 2.7 C_2H_6/Hf)

[a] Conditions: 135 mg of $Hf(CH_2tBu)_4$ (292 μmol) and 0.50 g of silica (230 μmol of ≡SiOH).

Scheme 1. Reaction of $Hf(CH_2tBu)_4$ with $SiO_{2-(800)}$ To Give $(\equiv SiO)Hf(CH_2tBu)_3$ (1-$SiO_{2-(800)}$)

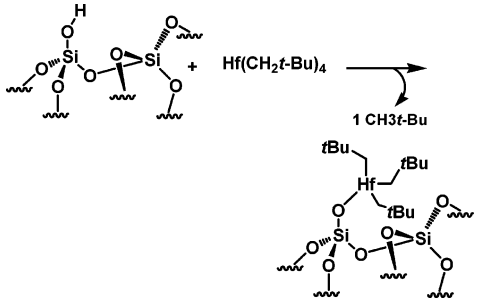

$SiO_{2-(500)}$[4] shows that the Hf−O (1.947(7) Å) and Hf−C (2.191-(7) Å) bonds, as well as the angle Hf−C_α−C_β (138°), are slightly smaller than the Zr−O (1.956(3) Å) and Zr−C (2.219-(4) Å) bonds and angle. It is generally reported that bond lengths obtained for 5d metal complexes are shorter than those of 3d metal complexes.[31,35]

In conclusion, the analytical data of the reaction of Hf-$(CH_2tBu)_4$ with $SiO_{2-(800)}$ indicate that three neopentyl ligands are linked to the hafnium center and that the ratio Hf/(≡SiOH) ≈ 1, which are consistent with the formation of a *unique surface species*, $(\equiv SiO)Hf(CH_2tBu)_3$ (**1**), *in only one surface environment* (Scheme 1).

Reactivity of $Hf(CH_2tBu)_4$ with Silica Dehydroxylated at 500 °C ($SiO_{2-(500)}$). Reactions of $SiO_{2-(800)}$ with both Zr-$(CH_2tBu)_4$ and $Hf(CH_2tBu)_4$ lead to the unique surface species $(\equiv SiO)M(CH_2tBu)_3$. The limitation of using $SiO_{2-(800)}$ is the low metal loading (Zr, 1.6%; Hf, 3.5%), since only the surface silanols (≡Si−OH) react with $M(CH_2tBu)_4$.

In the case of $SiO_{2-(500)}$, $Zr(CH_2tBu)_4$ also affords a unique surface species, $(\equiv SiO)Zr(CH_2tBu)_3$, with a loading of 3.1% instead of 1.6%.[30] To increase the Hf loading, we have studied the reaction of $Hf(CH_2tBu)_4$ with $SiO_{2-(500)}$.

The reaction of $Hf(CH_2tBu)_4$ with $SiO_{2-(500)}$ was carried out using the workup previously reported.

As expected, the loading in Hf is higher: 5% instead of 3.5%. The ratio C/Hf is also lower than in the case of $SiO_{2-(800)}$, and the quantity of gas evolved during the grafting and the hydrogenolysis is not consistent with a monografted species (Table 2). All this information suggests that the reaction does not lead to a unique surface species.

When $Hf(CH_2tBu)_4$ was sublimed onto $SiO_{2-(500)}$, the infrared band ascribed to isolated silanols, ν(Si−OH), at 3747 cm^{-1} disappeared totally (Figure 6). The broad band at 3700 cm^{-1} was still there and vibration bands characteristic of the neopentyl ligand appeared at 2955 ($\nu_{as}(CH_3)$), 2867 ($\nu_s(CH_3)$), 1466 (δ_{as}-(CH_3)), and 1364 cm^{-1} ($\delta_s(CH_3)$). Note that the same bands are observed when $Zr(CH_2tBu)_4$ is grafted onto $SiO_{2-(500)}$.

The band at 3700 cm^{-1} is consistent with the presence of interacting surface silanols.

The ^1H MAS NMR spectrum (Figure 7i) shows one very broad peak (Δ = 200 Hz) centered at 0.8 ppm attributed to the overlapping of two resonances: one due to the protons of the methyl groups $Hf(CH_2C(CH_3)_3)$ and one due to the remaining surface silanols at 1.8 ppm. The solid-state ^{13}C CP-MAS NMR spectrum (Figure 7ii) exhibits three different peaks at 34, 95, and 106 ppm. Peaks at 34 and 106 ppm have already been attributed respectively to the methyl groups and the secondary carbon of the neopentyl ligand of the monografted species complex $(\equiv SiO)Hf(CH_2tBu)_3$ (**1**-$SiO_{2-(500)}$). The presence of a broad peak at 95 ppm corroborates the fact that a second surface species has been formed.

The presence of two oxygen atoms in the coordination sphere of the metal leads to an upfield shift of the resonance of δ-$(M(CH_2C(CH_3)_3))$, in molecular complexes [(or (t-Bu_3SiO)Ta-$(CH_2C(CH_3)_3)_2(CHC(CH_3)_3)$, $\delta(M(CH_2C(CH_3)_3))$ 97.0 ppm; for (t-$Bu_3SiO)_2Ta(CH_2C(CH_3)_3)(CHC(CH_3)_3)$, $\delta(M(CH_2C(CH_3)_3)$ 73.9 ppm)[29] as well as in surface complex species ($(\equiv SiO)Zr$-$(CH_2tBu)_3$, $\delta(Zr(CH_2C(CH_3)_3))$ 96 ppm; $(\equiv SiO)_2Zr(CH_2tBu)_2$, $\delta(Zr(CH_2C(CH_3)_3)$, 87 ppm).[40a]

The peak at 95 ppm could correspond to the resonance of the secondary carbon of a bis-grafted species, $(\equiv SiO)_2Hf$-$(CH_2tBu)_2$ (**2**-$SiO_{2-(500)}$). This resonance is broad, due to a slight structural disorder leading to chemical shift anisotropy.[40b,c] Since this anisotropy is the consequence of the presence of different Si atoms, a disiloxy species bonded to two Si atoms will have a broader resonance than a monosiloxy one.

The deconvolution of the two different peaks allows an estimation of the ratio **1**-$SiO_{2-(500)}$/**2**-$SiO_{2-(500)}$ to be ca. 70/30 (Figure 8).

The combined analyses of the experimental data collected on the reaction of $Hf(CH_2tBu)_4$ with $SiO_{2-(500)}$ indicates the presence of two surface species mono- and bis-grafted to the silica surface and surrounded by three and two neopentyl ligands, respectively, $(\equiv SiO)Hf(CH_2tBu)_3$ (**1**-$SiO_{2-(500)}$) and $(\equiv SiO)_2Hf(CH_2tBu)_2$ (**2**-$SiO_{2-(500)}$), in the proportion 70/30. These proportions are in agreement with other experimental data (elemental analyses and quantification of the gas evolved) (Table 3).

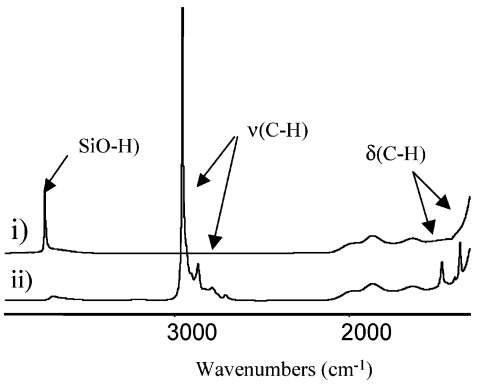

Figure 6. IR spectra: (i) $SiO_{2-(500)}$; (ii) sample after sublimation of $Hf(CH_2tBu)_4$ at 70 °C followed by vacuum treatment (10^{-5} Torr) at 70 °C for 1 h.

(40) (a) Wang, X.-X.; Veyre, L.; Lefebvre, F.; Patarin, J.; Basset, J.-M. *Microporous Mesoporous Mater*. **2003**, *66*, 169−179. (b) Casard, S.; Lesage, A.; Emsley, L. *J. Am. Chem. Soc*. **2005**, *127*, 4466−4476. (c) Sakellariou, D.; Brown, S. P.; Lesage, A.; Hediger, S.; Bardet, M.; Meriles, C. A.; Pines, A.; Emsley, L. *J. Am. Chem. Soc*. **2003**, *125*, 4376−4380.

(41) Clark, M.; Cramer, R. D., III; Van Opdenbosch, N. *J. Comput. Chem.* **1989**, *10*, 982−1012.

(42) Steward, J. J. P. *J. Comput. Chem.* **1991**, *10*, 320.

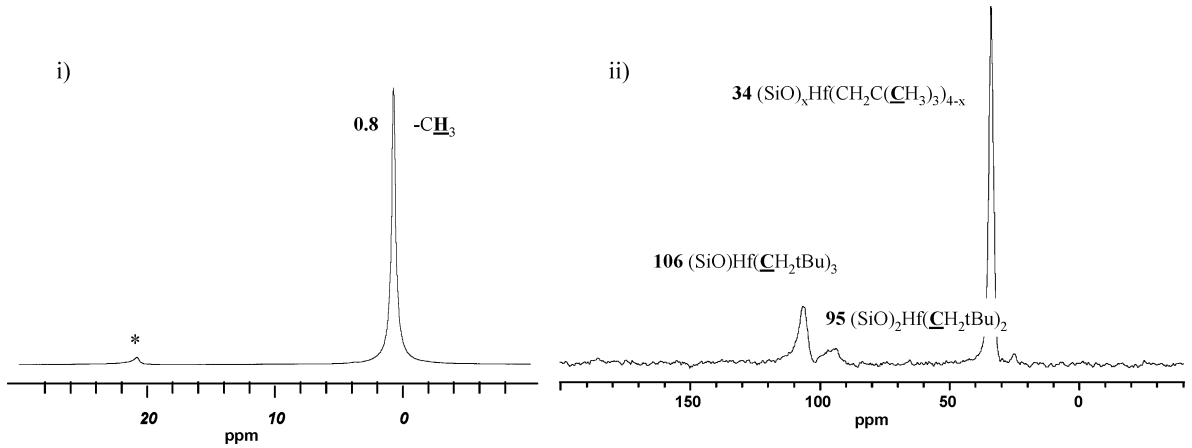

Figure 7. NMR spectra of Hf(CH$_2$*t*Bu)$_4$/SiO$_{2-(500)}$: (i) ^{1}H MAS; (ii) ^{13}C CP-MAS (the asterisk indicates a spinning sideband).

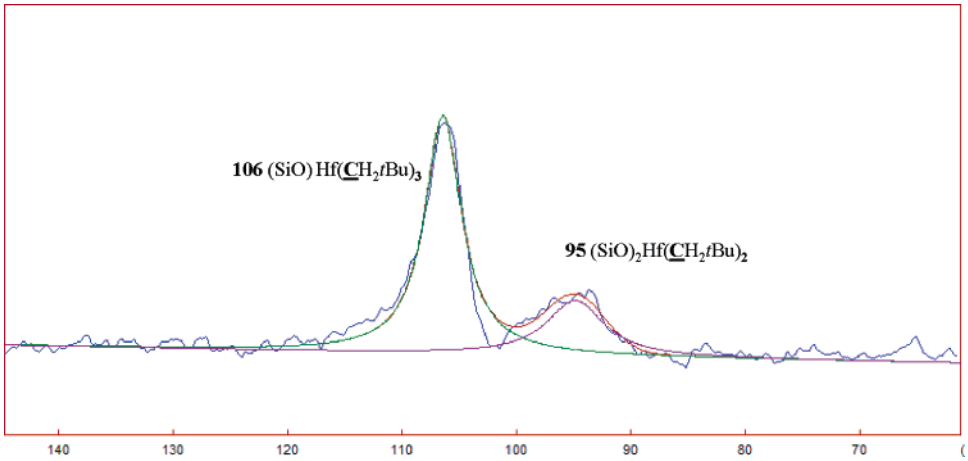

Figure 8. Deconvolution of the NMR spectrum of Hf(CH$_2$*t*Bu)$_4$/SiO$_{2-(500)}$.

Table 3. Grafting of Hf(CH$_2$*t*Bu)$_4$ onto SiO$_{2-(500)}$: Hydrolysis and Hydrogenolysis Experimental Results vs Theory

	nb ≡SiOH, nm^{-2}	nb Hf, nm^{-2}	wt % Hf	Hf(≡SiOH)	C/Hf	CH$_3$*t*Bu/Hf grafting	CH$_3$*t*Bu*/Hf hydrogenolysis
exptl	1.4	0.8	5.0	0.6 ± 0.1	12 ± 2	1.3 ± 0.1	2.8 ± 0.2
theory		1.2	7.2	0.9	13.7	1.3	2.7

The molecular modeling of **1**, performed using the Sybyl computer modeling program,[41,42] indicates that the projected area of **1** is 0.87 nm^2. This means the highest loading would be 1.15 Hf/nm^2: i.e., 6.5 Hf wt % if all of the free silanols were homogeneously spread on the surface. On SiO$_{2-(500)}$, the amount of silanol groups is 1.4 ± 0.1 OH nm^{-2}. Consequently, with this hypothesis, only 80% (1.15/1.4) of the ≡SiOH groups react with Hf(CH$_2$*t*Bu)$_4$.

However, since it is well-known that the dehydroxylation is statistical and leads to a nonhomogeneous distribution of silanols, we must expect a much lower value. Instead of the expected 6.5 Hf wt %, the experimental loading is 5.0% (80% of the theoretical value). The analytical data indicate that the ratio **1**-SiO$_{2-(500)}$/**2**-SiO$_{2-(500)}$ is ca. 70/30; this means that there is further reaction of 30% of **1**-SiO$_{2-(500)}$ with the 35% of unreacted ≡SiOH to form the disiloxy complex **2**-SiO$_{2-(500)}$. At the end, 85% of the surface ≡SiOH groups have been consumed. The presence of residual ≡SiOH (ca. 15%) was confirmed by the presence of a peak at 1.8 ppm in ^{1}H solid-state NMR spectroscopy and by the in situ IR experiment, with ν(Si−OH) at 3700 cm^{-1}.

Zr(CH$_2$*t*Bu)$_4$ reacts with SiO$_{2-(500)}$ to lead to the formation of *a unique monopodal species*, (≡SiO)Zr(CH$_2$*t*Bu)$_3$ (Scheme 2).[4] In contrast, the reaction of Hf(CH$_2$*t*Bu)$_4$ with SiO$_{2-(500)}$ afforded two surface species mono- and bis-grafted to the silica surface: (≡SiO)Hf(CH$_2$*t*Bu)$_3$ (**1**-SiO$_{2-(500)}$) and (≡SiO)$_2$Hf(CH$_2$*t*Bu)$_2$ (**2**-SiO$_{2-(500)}$), in the proportion 70/30. This difference in reactivity between Hf(CH$_2$*t*Bu)$_4$ and Zr(CH$_2$*t*Bu)$_4$ can be explained by two factors: the higher oxophilicity of the hafnium atom and the higher steric hindrance in the coordination sphere of hafnium, as proved by the EXAFS results.

Scheme 2. Reaction of M(CH$_2$*t*Bu)$_4$ (M = Zr, Hf) with SiO$_{2-(500)}$

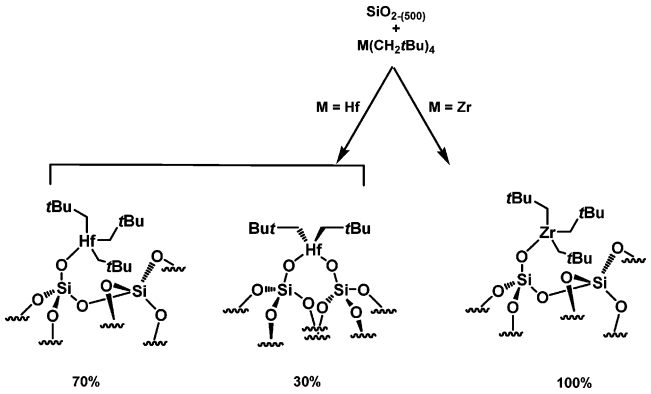

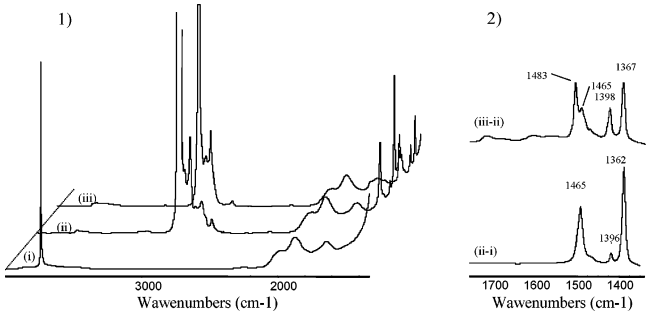

Figure 9. (1) Reaction of (≡SiO)Hf(CH_2tBu)$_3$ with O_2 monitored by IR spectroscopy: (i) $SiO_{2-(800)}$; (ii) (≡SiO)Hf(CH_2tBu)$_3$; (iii) sample after reaction with oxygen. (2) Enlargement of the 1700−1300 cm^{-1} spectral region of (1).

Table 4. IR Data (cm^{-1}) for (≡SiO)M(CH_2tBu)$_3$ and (≡SiO)M(OCH_2tBu)$_3$ (M = Zr, Hf)

(≡SiO)Hf(CH_2tBu)$_3$		(≡SiO)Zr(CH_2tBu)$_3$	
alone	+O_2	alone	tBuCH$_2$OH
1362	1367	1363	1366
1396	1398	1392	1398
1465	1465	1466	1466
	1483		1481

Reactivity of (≡SiO)Hf(CH_2tBu)$_3$ (1-$SiO_{2-(800)}$) with Dry Oxygen. The *unique surface species in only one surface environment* (≡SiO)Hf(CH_2tBu)$_3$ (**1**-$SiO_{2-(800)}$) could be the starting complex to generate other (and more chemically stable) well-defined surface species. For instance, the M−C bond could be replaced by more stable M−O bonds. Subsequently, we undertook the study of the reaction of **1**-$SiO_{2-(800)}$ with dry oxygen and compared the data to those obtained with well-defined grafted Zr complexes.[43]

When dry oxygen is added at 25 °C to **1**-$SiO_{2-(800)}$, there is no gas evolution. The reaction is very exothermic, but the elemental analysis indicates no change in the amount of Hf and C compared to that in **1**-$SiO_{2-(800)}$. When this reaction is monitored by infrared spectroscopy, peaks at 1362, 1396, and 1465 cm^{-1} are spontaneously replaced by bands at 1367, 1398, 1465, and 1483 cm^{-1} (Figure 9). The same changes were observed during the reaction of (≡SiO)Zr(CH_2tBu)$_3$ with neopentyl alcohol.[43] Peaks at 1363, 1392, and 1466 cm^{-1} were replaced by new ones at 1366, 1398, 1481, and 1466 cm^{-1} (Table 4).

The ^{1}H NMR spectrum (Figure 10) of **1**-$SiO_{2-(800)}$ under oxygen shows a peak at 1.2 ppm and a new broad signal centered at 3.6 ppm. The ^{13}C CP-MAS NMR spectrum presents three peaks at 25, 33, and 82 ppm. By comparison with the ^{13}C NMR spectrum of molecular Hf(OCH_2tBu)$_4$, resonances at 3.6 ppm in ^{1}H NMR and 83 ppm in ^{13}C NMR are assigned to the proton and to the carbon of the CH_2 group bonded to the oxygen. The other peaks at 25 and 33 ppm are attributed to the methyl groups CH_3 and the quaternary carbon, respectively. The peak at 1.2 ppm in ^{1}H NMR is attributed to the protons of the methyl groups. In the ^{13}C CP MAS NMR spectrum of (≡SiO)Zr(CH_2tBu)$_3$ under oxygen or neopentyl alcohol, the peak corresponding to the methyl groups is shifted from 34 to 25 ppm and the peak attributed to the secondary carbon from 95.5 to 82 ppm.[43] As with Hf complexes the quaternary carbon atom at 33 ppm is only observed in the spectrum of the oxidized product. By comparison with the zirconium chemistry, the reaction of **1**-$SiO_{2-(800)}$ with O_2 leads to the unique species (≡SiO)Hf(OCH_2tBu)$_3$ (**3**).

When **3** is heated to 250 °C, no neopentane or other alkanes were detected in the gas phase, and the results of the elemental analysis were similar (3.1 wt % C) to those of the starting material (3.2 wt % C); consequently, (≡SiO)Hf(OCH_2tBu)$_3$ is stable up to 250 °C. In contrast, the reaction of **3** with H_2O at room temperature led to a drastic decrease of C wt % from 3.1 to 0.3.

In conclusion, the reaction of (≡SiO)Hf(CH_2tBu)$_3$ with oxygen at room temperature, as in the case of (≡SiO)Zr(CH_2tBu)$_3$ leads to the transformation of the three neopentyl ligands into neopentoxy ones and to the formation of a unique surface species (≡SiO)Hf(OCH_2tBu)$_3$, **3** stable up to 250 °C (Scheme 3).

Thermal Stability of (≡SiO)Hf(CH_2tBu)$_3$ (1-$SiO_{2-(800)}$). The thermal stability of **1**-$SiO_{2-(800)}$ was first monitored by in situ infrared spectroscopy and then investigated under two different experimental procedures: (i) in a batch reactor and (ii) in a tubular continuous reactor.

(a) In Situ IR Spectroscopy. For the in situ infrared study,

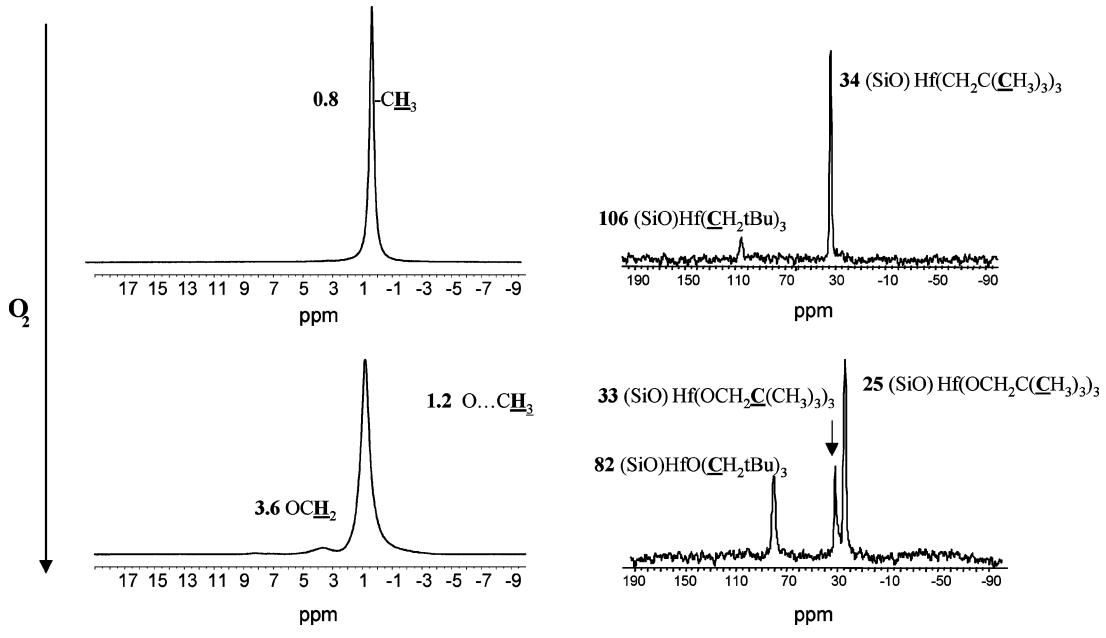

Figure 10. Solid-state NMR ^{1}H MAS and ^{13}C CP-MAS spectra of **1**-$SiO_{2-(800)}$ before and after oxidation.

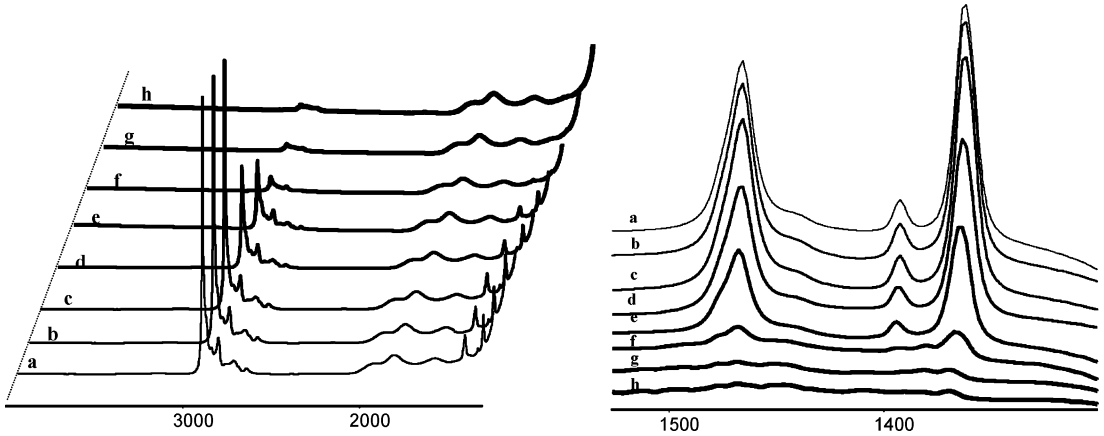

Figure 11. Infrared spectra of **1** as a function of the thermolysis temperature in the 3800−1200 cm^{-1} region and the 1500−1300 cm^{-1} extended region: (a) 25 °C; (b) 50 °C; (c) 100 °C; (d) 150 °C; (e) 200 °C; (f) 250 °C; (g) 300 °C; (h) 350 °C.

Scheme 3. Reactivity of 1-SiO$_{2-(800)}$ with Oxygen

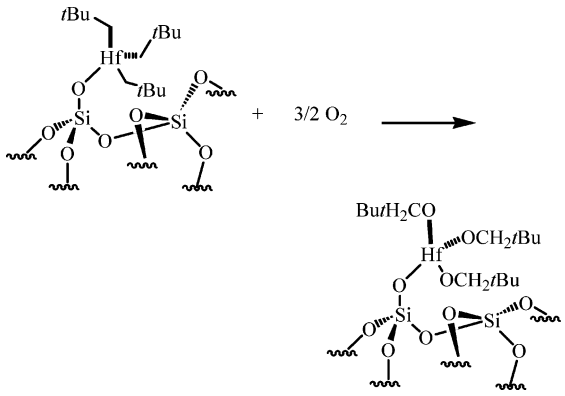

the silica pellet of **1**-SiO$_{2-(800)}$ was heated to 350 °C under argon pressure (500 Torr) with a temperature slope of 50 °C h^{-1}. The corresponding spectra of the solid are depicted in Figure 11. The gas phase was also analyzed by GC.

There are few changes in the spectra (Figure 11a−c) until the temperature reaches 100 °C; a decrease of the intensity of the peaks (less than 2%) is observed (difference of peak area of spectra c−a). From 150 to 250 °C, there is a continuous decrease of the intensity of the peaks due to the vibrations ν(CH) and δ(CH) (Figure 11d−f). The intensity of these peaks reaches a minimum (4% of the starting value) at 250 °C, which stays constant up to 350 °C (Figure 11g,h).

Concurrently, the gas phase was analyzed by infrared and GC. Up to 150 °C, the gas phase contains only traces of neopentane and, at 150 °C, neopentane and methane. Above this temperature, GC data indicate the formation, in addition to the previous alkanes, of isobutene.

This infrared study shows that **1**-SiO$_{2-(800)}$ under argon is stable up to 150 °C and totally decomposes at 250 °C. However, even for temperatures up to 350 °C, the infrared spectra exhibit some weak peaks in the ν(C(sp^3)−H) region. To quantify the evolved gas, the thermolysis of **1**-SiO$_{2-(800)}$ has been performed in a batch reactor.

(b) Thermolysis of (≡SiO)Hf(CH$_2$tBu)$_3$ (1) in a Batch Reactor, under Static Vacuum. The experiment was carried out on several samples of **1**-SiO$_{2-(800)}$ loaded at ca. 3.3% in Hf. At room temperature, the sample was evacuated under 10^{-5} mmHg, and then the sample was heated over 2 h to 150 or 250 °C and maintained at this temperature for 20 h. At this point the sample was cooled to 25 °C and the gas phase was analyzed by GC. The solid sample was then evacuated at room temperature and analyzed by solid-state ^{1}H MAS and ^{13}C CP-MAS NMR, by elemental analysis, and by reaction with water.

At 150 °C, only traces of alkanes (neopentane C$_5$, methane C$_1$, and isobutene iC$_4$=) are formed, corresponding to an overall loss of 1 C per Hf surface atom. The NMR spectra of **1**-SiO$_{2-(800)}$ before and after thermolysis are equivalent (Figure 12 a,b). These results confirmed those of the infrared study and confirmed that **1**-SiO$_{2-(800)}$ is stable up to 150 °C.

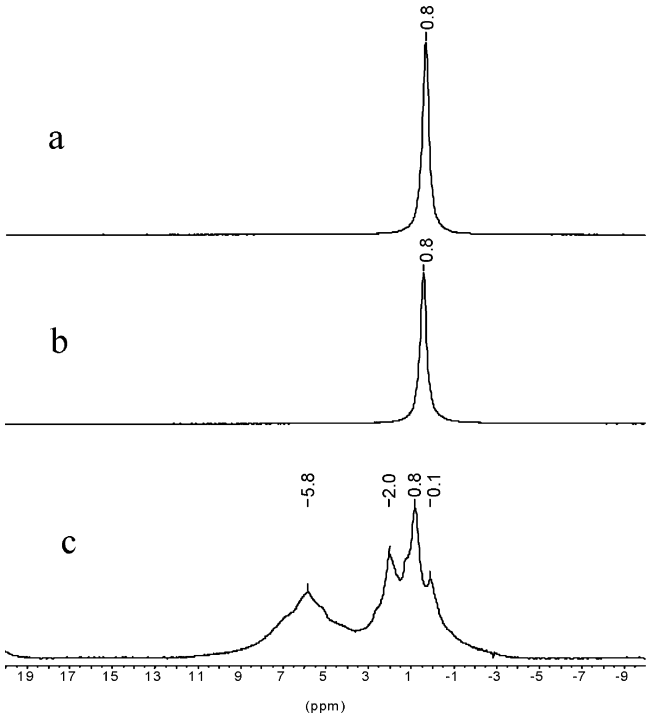

Figure 12. ^{1}H MAS NMR spectra: (a) **1**-SiO$_{2-(800)}$; (b) **1**-SiO$_{2-(800)}$ treated at 150 °C; (c) **1**-SiO$_{2-(800)}$ treated at 250 °C.

At 250 °C, the solid became brown and alkanes were evolved, with an overall loss of 5.4 ± 0.2 C per grafted Hf: i.e., one ligand −CH$_2$tBu (C$_5$ (0.64 equiv), C$_1$ (1.39 equiv), ethane C$_2$ (0.22 equiv), propane C$_3$ (0.14 equiv), and isobutane iC$_4$ (0.03 equiv)].

The hydrogenolysis and the hydrolysis of the residual brown powder led to the evolution of a small amount of volatile hydrocarbons, mainly C$_1$, iC$_4$=, 1-butene, isopentene iC$_5$=, and

(43) Adachi, M.; Nedez, C.; Wang, X. X.; Bayard, F.; Dufaud, V.; Lefebvre, F.; Basset, J.-M. *J. Mol. Catal. A* **2003**, *204−205*, 443−455.

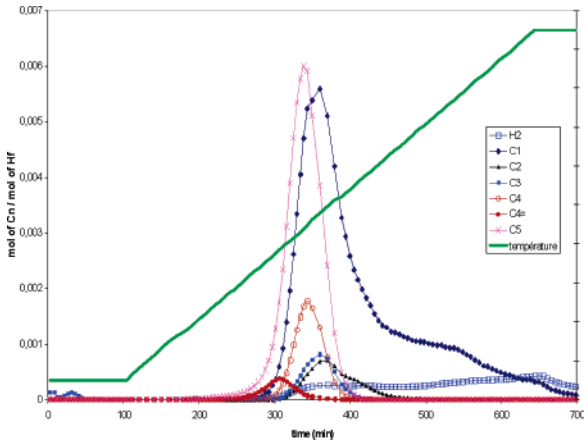

Figure 13. Instantaneous moles of Cn evolved per mole of grafted hafnium as a function of the time during the thermolysis of **1**-$SiO_{2-(800)}$ from 25 to 475 °C (50 °C h^{-1}).

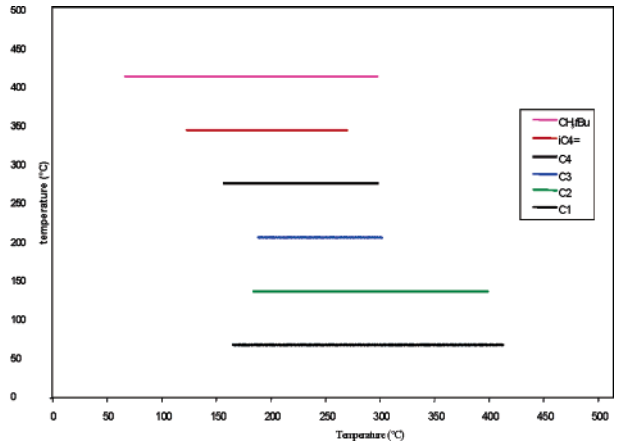

Figure 14. Temperature range of the forrmation of alkanes and alkenes during the thermolysis of **1**-$SiO_{2-(800)}$ from 25 to 475 °C (50 °C h^{-1}).

two hydrocarbons C_n ($n \geq 5$) (1.3 ± 0.2 C per grafted Hf). Consequently, after thermolysis of **1**-$SiO_{2-(800)}$ at 250 °C, there is no longer a neopentyl group linked to the hafnium atom. However, the total amount of evolved gas does not correspond to the loss of three neopentyl groups.

The low amount of evolved gas is not due to a partial oxidation of **1**-$SiO_{2-(800)}$, because the oxide species (≡SiO)-$Hf(OCH_2tBu)_3$ (**3**) is stable up to 250 °C and its ^{13}C NMR spectra stayed unchanged. However, in the ^{13}C NMR spectrum of **1**-$SiO_{2-(800)}$ treated at 250 °C no peak at 83 ppm corresponding to the $-OCH_2tBu$ group is detected. Moreover, the ^1H NMR spectrum of (≡SiO)$Hf(CH_2tBu)_3$ treated at 250 °C (Figure 12c) shows new peaks at 0.1, 2, and 5.8 ppm which could be attributed to the protons of the remaining methyl groups on the surface ($CH_2C(CH_3)_3$, $CH_2C(CH_3)_3$) and the peak at 5.8 ppm to the protons of polymeric material. (the ^1H NMR spectrum of [Hf]−H + isobutene exhibits a similar broad peak around 5−6 ppm).

(c) Thermal Stability of 1-$SiO_{2-(800)}$ in a Continuous Tubular Reactor, under Argon. The thermal stability of **1**-$SiO_{2-(800)}$ has also been studied in a continuous tubular reactor flushed by argon. The temperature slope is 50 °C h^{-1}, and the maximal temperature is 475 °C. The gases evolved were analyzed continuously by GC. The instantaneous amount of gas evolved during the experiment is given in Figure 13. Another type of plot is useful to visualize the temperature ranges of C_n formation, given in Figure 14. This experiment indicates that there is no gas evolution when the temperature is below 65 °C.

Between 65 and 110 °C only neopentane, C_5, was detected. The formation of C_5 was observed until Θ = 298 °C. The overall final ratio of evolved C_5 per grafted Hf was 1.

Above 110 °C $iC_{4=}$ is evolved in addition to C_5. Above 150 °C, iC_4 and C_1 appeared in the gas phase, and then C_3 and C_2 appeared consecutively at 161 and 165 °C. Above 413 °C, only H_2 was formed. The experiment was stopped at 475 °C. At this stage 1.05 C_5, 1.92 C_1, 0.06 $iC_{4=}$, 0.26 iC_4, 0.17 C_2, 0.15 C_3, and 0.36 H_2 are produced, i.e. 9.2 ± 0.5 C (two $-CH_2tBu$ ligands) per grafted Hf, and the elemental analysis of the residual solid indicates that the ratio of the residual C on the surface per grafted Hf was equal to 6.5 ± 0.5. Therefore, all carbons from **1**-$SiO_{2-(800)}$ are recovered (9.2 + 6.5 = 15.7 ± 0.5 for 15). EPR data indicate that there is less than 3% of $[Hf]^{3+}$ in the residual solid.

The formation of C_5 could proceed either intramolecularly between two neopentyl groups via α-H abstraction and reductive elimination or via γ-H abstraction and reductive elimination of

Scheme 4. Decomposition Pathways of 1-$SiO_{2-(800)}$ below 110 °C

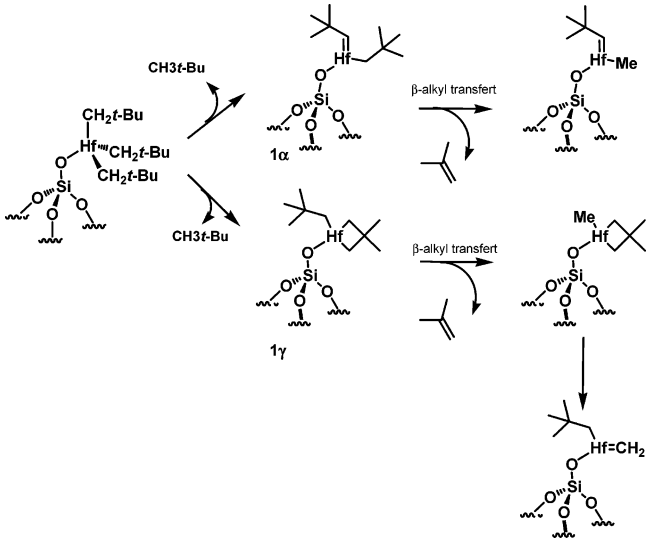

neopentane to form either a neopentylidene complex **1**α or the hafnacyclobutane intermediate **1**γ (Scheme 4).[22,44] The first reaction step in the thermolysis of tetraneopentyl complexes of group 4 has been studied by calculations and chemical vapor deposition with deuterium-labeled neopentyl-d_2 [Me_3CCD_2] ligands. The results clearly support a mechanism in which γ-H abstraction was the major first step of the thermolysis for the Zr and Hf derivatives, in contrast to the case for Ti derivatives, where the α-H abstraction was more favorable.[22,44,45]

The formation of $iC_{4=}$ can be explained by a β-methyl elimination reaction in the coordination sphere of the metal. The evolution of $iC_{4=}$ leads to the formation of a Hf−Me bond (Scheme 4).[23,46] The Hf complexes are known to have a high tendency to undergo β-alkyl transfer because of the sterically very demanding neopentyl ligand (vide supra).

After 300 min (i.e. above 250 °C) the formation of iC_4 (200−240 °C), C_3 (210−260 °C), C_1 (175−400 °C), and H_2 (above 210 °C) is observed. As previous results proved that hafnium

(44) Cheon, J.; Dubois, L. H.; Girolami, G. S. *J. Am. Chem. Soc.* **1997**, *119*, 6814−6820.
(45) Wu, Y.-D.; Peng, Z.-H.; Xue, Z. *J. Am. Chem. Soc.* **1996**, *118*, 9772−9777.
(46) Lin, M.; Spivak, G. J.; Baird, M. C. *Organometallics* **2002**, *21*, 2350−2352.

Scheme 5. Hydrogenolysis of Neopentane

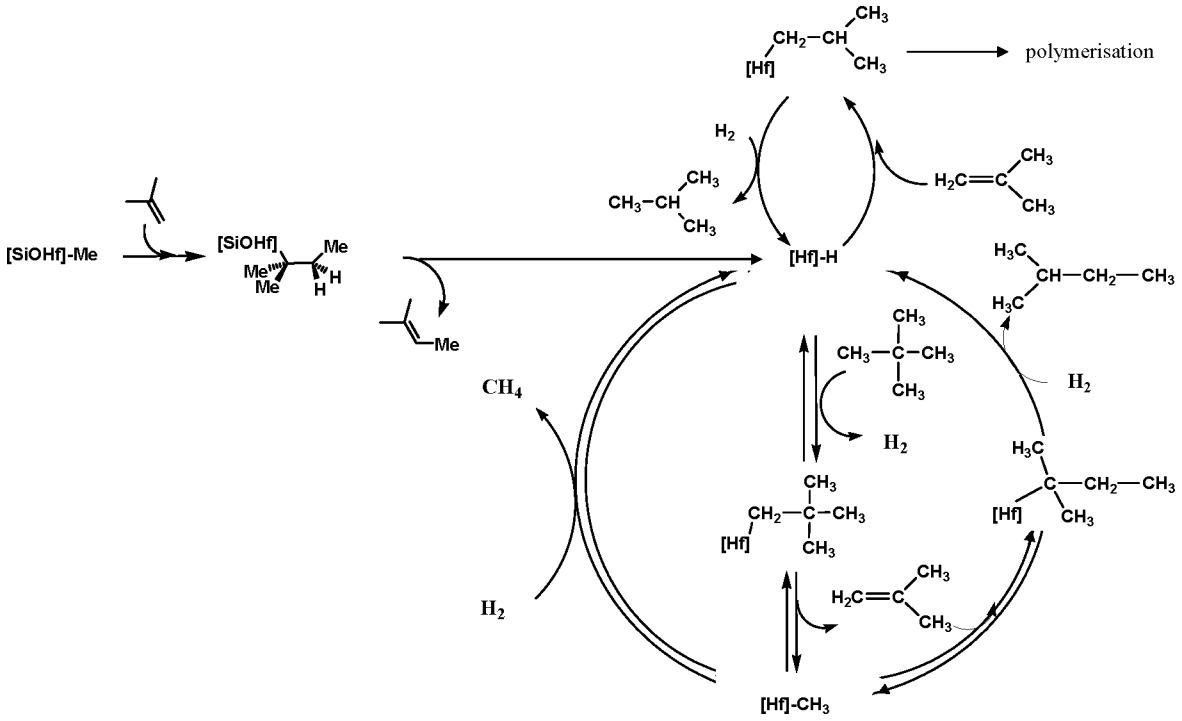

Scheme 6. Insertion of Isobutene in the [Hf]−Me Bond

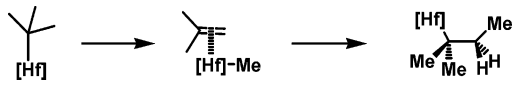

hydrides are active in neopentane hydrogenolysis,[15] the formation of alkanes can be explained through the hydrogenolysis reaction of alkyl ligands bonded to the metal (Scheme 5). If so, this reaction required the presence, even as an intermediate, of a hafnium hydride surface complex [Hf]−H.[15] Furthermore, when the thermolysis of **1**-SiO$_{2-(800)}$ at 250 °C was quenched with water, the presence of several C_5 species, in particular $iC_{5=}$ and probably some C_n ($n \geq 5$) (unidentified), has been demonstrated. The formation of these hydrocarbons C_n ($n \geq 5$) could be due to the insertion of $iC_{4=}$ into a Hf−R bond, leading to an Hf−C(CH$_2$R)Me$_2$ bond.[12,38] Then, via a β-H elimination there is formation of the observed alkenes C_n ($n \geq 5$) and a [Hf]−H surface complex. At this step hafnium hydride surface complex can react with any alkane and generate H_2 and a new Hf−R surface complex. For instance, the insertion of $iC_{4=}$ into an Hf−Me bond leads through a β-H elimination to $iC_{5=}$.

Note that the EPR spectrum indicated the presence of reduced Hf in the sample (∼3%); therefore, a reductive elimination process can generate these higher alkanes. However, this route is estimated to be highly endothermic in the group 4 compounds.[16] In contrast, β-H elimination would be expected to be favorable, since the resulting hydride [Hf]−H is predicted to be ca. 10 kcal mol^{-1} more stable than the alkyl complex [Hf]−R.[18]

Comparison of the Thermal Treatment of (≡SiO)Zr(CH$_2$tBu)$_3$ and 1-SiO$_{2-(800)}$. The evolution of the area of the ν(CH) bands with temperature during thermolysis under vacuum of **1**-SiO$_{2-(800)}$ and (≡SiO)Zr(CH$_2$tBu)$_3$ proves that (≡SiO)Zr(CH$_2$tBu)$_3$ has a lower thermal stability than **1**-SiO$_{2-(800)}$ (Figure 15).

For both complexes the nature of the gases evolved during the thermolysis is quite similar. First C_5 and then C_1 and other alkanes (iC_4, $iC_{4=}$, C_2, and C_3) are evolved. A more detailed analysis indicates that with zirconium surface complexes there is almost no isobutene evolved, whereas with hafnium derivatives, a significant amount of this gas can be detected. Interestingly, in the case of hafnium, isopentene is observed, but this is not the case with zirconium. This suggests that isobutene coming from β-alkyl transfer on Hf is inserted in the Hf−Me bond (from the β-methyl transfer) (Scheme 6).

However, there are two main differences: the range of gas evolution (between 80 and 190 °C for (≡SiO)Zr(CH$_2$tBu)$_3$ and between 65 and 413 °C for **1**-SiO$_{2-(800)}$), and the ratio C_5/C_1, which varies from 1.4 to 0.27 for Zr and Hf, respectively (Figure 16). This last result emphasizes the fact that the surface hafnium complex is more active in alkane hydrogenolysis[15,19] and in olefin polymerization.

Conclusion

As with Zr(CH$_2$tBu)$_4$, Hf(CH$_2$tBu)$_4$ reacts with SiO$_{2-(800)}$ to afford a *unique surface species with only a single surface environment*, (≡SiO)Hf(CH$_2$tBu)$_3$ (**1**-SiO$_{2-(800)}$). In contrast, in the case of SiO$_{2-(500)}$ two *surface species*, **1**-SiO$_{2-(500)}$ and (≡SiO)$_2$Hf(CH$_2$tBu)$_2$ (**2**-SiO$_{2-(500)}$), are formed instead of only one in the case of the zirconium species (≡SiO)Zr(CH$_2$tBu)$_3$.

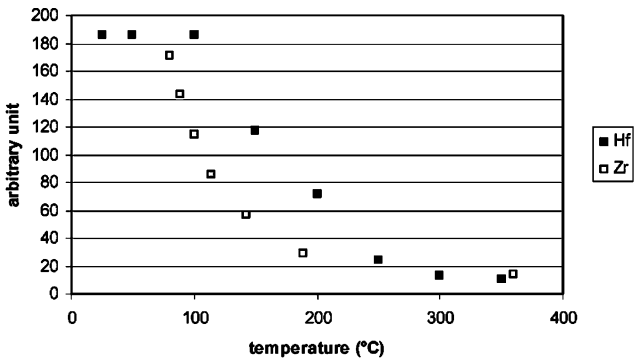

Figure 15. Evolution of the area of ν(CH) bands of **1**-SiO$_{2-(800)}$ and (≡SiO)Zr(CH$_2$tBu)$_3$ versus the temperature of thermolysis.

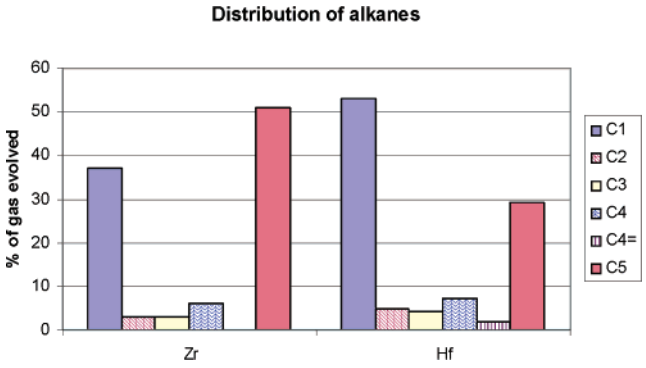

Figure 16. Distribution of gases evolved during the thermolysis of (≡SiO)M(CH_2tBu)$_4$.

A comparison of the analytical data of **1**-$SiO_{2-(800)}$ and (≡SiO)-Zr(CH_2tBu)$_3$ indicates, in EXAFS, shorter Hf−C and Hf−O bonds, a larger Hf−C_α−C_β angle, and, in 2D *J*-resolved spectra, a lower $^1J(C_\alpha-H)$ value for the hafnium complex compared to that for the zirconium complex. These differences underline a greater steric hindrance in the coordination sphere of the Hf metal. Thermolysis experiments prove that **1**-$SiO_{2-(800)}$ is more stable and more active in alkane hydrogenolysis than (≡SiO)-Zr(CH_2tBu)$_3$.

Experimental Section

All experiments were carried out by using standard air-free methodology in an argon-filled Vacuum Atmospheres glovebox, on a Schlenk line, or in a Schlenk-type apparatus interfaced to a high-vacuum line (10^{-5} Torr). Pentane, hexane, THF, and ether were purified according to published procedures,[47] stored under argon over 3 Å molecular sieves, and degassed prior to use. C_6D_6 (SDS) was distilled over Na/benzophenone.

$HfCl_4$ (Cezus, 270 ppm of Zr), was used as received. Neopentyllithium was prepared from neopentyl chloride (SAFC 99%, stored under argon over 3 Å molecular sieves**)** and Li wire **(**Aldrich, 98+%, 1% Na). Neopentylmagnesium chloride was prepared from neopentyl chloride (SAFC 99%, used as received) and Mg chips (Alfa Aesar 99%). Hydrogen was dried over a deoxo catalyst (BASF R3-11 + 4 Å molecular sieves) prior to use.

Gas-phase analyses were performed on a Hewlett-Packard 5890 Series II gas chromatograph equipped with a flame ionization detector and a KCl/Al_2O_3 on fused silica column (50 × 0.32 mm).

Elemental analyses were performed at the CNRS Central Analysis Department of Solaize, France, or at the LSEO of Dijon, France.

Infrared spectra were recorded on a Nicolet 550-FT spectrometer by using a custom infrared cell equipped with CaF_2 windows, allowing in situ studies. Typically, 16 scans were accumulated for each spectrum (resolution 2 cm^{-1}).

Solution NMR spectra were recorded on an Bruker AM-300 spectrometer. All of the chemical shifts were measured relative to residual ^1H or ^{13}C resonances in deuterated solvents: C_6D_6 δ 7.15 ppm for ^1H, 128 ppm for ^{13}C.

The ^1H MAS and ^{13}C CP-MAS NMR spectra were recorded on a Bruker DSX-300 or a Bruker Avance 500 spectrometer equipped with a standard 4 mm double-bearing probe head. Samples were introduced under argon in a zirconia rotor, which was then tightly closed. The spinning rate was typically 10 kHz. Typical cross-polarization sequences were used, with a 5 ms contact time and a recycle delay of 1−4 s to allow the complete relaxation of the ^1H nuclei. All chemical shifts are given with respect to TMS, as an external reference.

The two-dimensional *J*-resolved experiment was performed as previously described:[48] after cross-polarization from protons, carbon magnetization evolves during t_1 under proton homonuclear decoupling. Simultaneous 180° carbon and proton pulses are applied in the middle of t_1 to refocus the carbon chemical shift evolution, while the modulation is retained by the heteronuclear J_{CH} scalar couplings. A Z filter is finally applied to allow phase-sensitive detection in ω_1. Proton homonuclear decoupling was performed by using the frequency-switched Lee−Goldburg (FSLG) decoupling sequence.[49,50] Quadrature detection in ω_1 was achieved using the TPPI method.[51] The rotor spinning frequency was 10 kHz, in order to synchronize the t_1 increment with the rotor period. The proton RF field strength was set to 83 kHz during t_1 (FSLG decoupling) and acquisition (TPPM decoupling).[52] The lengths of carbon and proton 180° pulses were 5.4 (5.4) and 6 (6) μs, respectively, for (≡SiO)Hf(CH_2tBu)$_4$ ((≡SiO)Zr(CH_2tBu)$_4$). An experimental scaling factor, measured as already described,[53] of 0.52 was found, which gave a corrected spectral width of 2452 Hz in the ω_1 dimension. The recycle delay was 3 s (2 s), and a total of 75 (80) t_1 increments with 1024 (256) scans each were collected.

The X-ray absorption spectra were acquired at the SRS of the CCLRC at Daresbury, U.K., on beam line 7.1. The two samples studied, a solid resulting from the grafting of $HfNp_4$ on $SiO_{2-(800)}$ and a benzene solution of $HfNp_4$, were packaged within a nitrogen-filled drybox in a double-airtight sample holder equipped with Kapton windows. The samples were studied at room temperature at the hafnium L_{III} edge, in the transmission (solid) or fluorescence ($HfNp_4$ solution) mode, using a double-crystal Si-(111) monochromator detuned to eliminate most of the higher harmonics content of the beam, and the spectra were recorded between 9300 and 10 300 eV. The spectra analyzed were the result of the averaging of three acquisitions. The data analyses were performed by standard procedures using the programs developed by Alain Michalowicz, in particular the EXAFS fitting program RoundMidnight. Fitting of the spectrum was done on the k^3- and k^1-weighted data (a k^3 weighting is recommended, since only light backscatterers with $Z < 36$ are present), using the following EXAFS equation, where S_0^2 is a scale factor (determined from the spectrum of the $HfNp_4$ reference compound), N_i is the coordination number of shell i, r_c is the total central atom loss factor, F_i is the EXAFS scattering function for atom i, R_i is the distance to atom i from the absorbing atom, λ is the photoelectron mean free path, σ_i is the Debye−Waller factor, Φ_i is the EXAFS phase function for atom i, and Φ_c is the EXAFS phase function for the absorbing atom:

$$\chi(k) \cong S_0^2[r_c(k)]\sum_{i=1}^{n}\frac{N_i[F_i(k,R_i)]}{kR_i^2}\exp\left(\frac{-2R_i}{\lambda(k)}\right)\exp(-2\sigma_i^2k^2)\sin[2kR_i + \Phi_i(k,R_i) + \Phi_c(k)]$$

The program FEFF7 was used to calculate theoretical values for r_c, F_i, λ, and $\Phi_i + \Phi_c$ on the basis of model clusters of atoms.[54] The refinements were performed by fitting the structural parameters N_i, R_i, σ_i, and the energy shift ΔE_0 (the same for all shells). The fit residue, ρ (%), was calculated by the formula

(47) Perrin, D. D.; Armarego, W. L. F. *Purification of Laboratory Chemicals*, 3rd ed.; Pergamon: Oxford, U.K., 1988.

(48) Lesage, A.; Emsley, L.; Chabanas, M.; Coperet, C.; Basset, J.-M. *Angew. Chem., Int. Ed.* **2002**, *41*, 4535.

(49) Bielecki, A.; Kolbert, A. C.; Levitt, M. H. *Chem. Phys. Lett.* **1989**, *155*, 341.

(50) Levitt, M. H.; Kolbert, A. C.; Bielecki, A.; Ruben, D. J. *Solid State Nucl. Magn. Reson.* **1993**, *2*, 151.

(51) Marion, D.; Wuethrich, K. *Biochem. Biophys. Res. Commun.* **1983**, *113*, 967.

(52) Bennett, A. E.; Rienstra, C. M.; Auger, M. L., K. V.; Griffin, R. G. *J. Chem. Phys.* **1995**, *103*, 6951.

(53) Lesage, A.; Duma, L.; Sakellariou, D.; Emsley, L. *J. Am. Chem. Soc.* **2001**, *123*, 5747.

(54) Zabinsky, S. I.; Rehr, J. J.; Ankudinov, A.; Albers, R. C.; Eller, M. J. *Phys. Rev. B* **1995**, *52*, 2995−3009.

$$\rho = \frac{\sum_k [k^3[\chi_{exp}(k)] - k^3[\chi_{cal}(k)]]^2}{\sum_k [k^3[\chi_{exp}(k)]]^2} \times 100$$

As recommended by the Standards and Criteria Committee of the International XAFS Society,[55] an improvement of the fit took into account the number of fitted parameters (decrease of the quality factor, $(\Delta\chi)^2/\nu$, where ν is the number of degrees of freedom in the signal).

Preparation of Molecular)Precursors. Hf(CH$_2$*t*Bu)$_4$ and Zr(CH$_2$*t*Bu)$_4$ were prepared according to literature procedures.[27] The synthesis of Hf(CH$_2$*t*Bu)$_4$ was modified to allow the preparation of Hf(^{13}CH$_2$*t*Bu)$_4$ in better yield.

Synthesis of Tetraneopentylhafnium, Hf(^{13}CH$_2$*t*Bu)$_4$ (10%). *t*Bu^{13}CH$_2$MgCl was prepared according to literature procedures.[29]

In a glass reactor under argon, 10 mL of a 1 M solution of *t*Bu^{13}CH$_2$MgCl (10%; 10 mmol, 5.8 equiv) in diethyl ether/THF was added dropwise at 0 °C over a solution of hafnium tetrachloride, HfCl$_4$ (540 mg, 1.7 mmol), in diethyl ether. The mixture was stirred at room temperature overnight. After filtration, the solvent was removed under vacuum and 10 mL of dry pentane was introduced to extract the product. The solid was washed five times, and the solvent was evaporated under vacuum to leave a yellowish oil. Sublimation (70 °C, 10^{-5} Torr) afforded bright white crystals: 450 mg, 0.97 mmol, yield 57%. ^{1}H NMR (C_6D_6; δ, ppm): 1.17 (36, s, CH$_2$C(C*H*$_3$)$_3$), 0.9 (8, s, C*H*$_2$C(CH$_3$)$_3$). ^{13}C NMR (C_6D_6; δ, ppm): 117 (*C*H$_2$C(CH$_3$)$_3$), 36 (CH$_2$*C*(CH$_3$)$_3$), 35 (CH$_2$C(*C*H$_3$)$_3$).

Preparation of 1-SiO$_{2-(800)}$. (a) Impregnation Workup. A mixture of Hf(CH$_2$*t*Bu)$_4$ (166 mg, 360 μmol, 1.4 equiv) and SiO$_{2-(800)}$ (1.43 g, 256 μmol of OH) in pentane (10 mL) was stirred at 25 °C for 3 h. After filtration, the solid was washed three times with pentane and all volatile compounds were condensed into another reactor (of known volume) so as to quantify the neopentane evolved during the grafting. The resulting white powder was dried under vacuum (10^{-5} Torr) to yield 1.4 g of **1**. Gas analyses by chromatography indicate the formation of 300 ± 30 μmol of neopentane during the grafting (1.0 ± 0.1 CH$_3$*t*Bu/Hf, 1.0 ± 0.1 CH$_3$*t*Bu/(≡SiOH), 1.1 ± 0.1 Hf/(≡SiOH)). Elemental analyses of **1**-SiO$_{2-(800)}$: Hf, 3.5 wt %; C, 3.2 wt % (14 ± 2 C/Hf). Solid-state ^{1}H NMR (δ, ppm): 0.8. CP/MAS ^{13}C NMR (δ, ppm): 106 and 34.

(b) Sublimation Workup. A mixture of Hf(CH$_2$*t*Bu)$_4$ (53 mg, 114 μmol, 1.3 equiv) and SiO$_{2-(800)}$ (0.5 g, 90 μmol of OH) was stirred at 70 °C for 2 h. Pentane (10 mL) was introduced into the reactor by distillation, and the solid was washed three times. The resulting white powder was dried under vacuum (10^{-5} Torr) to yield 0.50 g of **1**-SiO$_{2-(800)}$. Elemental analyses of **1**-SiO$_{2-(800)}$: Hf, 3.2 wt %; C, 3.4 wt % (16 ± 2 C/Hf; 0.9 ± 0.1 Hf/(≡SiOH)). Solid-state ^{1}H NMR (δ, ppm): 0.8. CP/MAS ^{13}C NMR (δ, ppm): 106 and 34.

Oxidation. Oxidation was performed under strict exclusion of air, using standard break-seal glass apparatus. Oxygen (500 mbar) was dried over molecular sieves prior to use. The reaction was monitored by IR and ^{1}H MAS and ^{13}C CP-MAS NMR spectroscopy.

Hydrogenolysis. Hydrogenolysis was performed under strict exclusion of air, using standard break-seal glass apparatus. Hydrogen (500 mbar) was dried over molecular sieves and deoxo catalyst (BASF R3−11 + 4 Å molecular sieves) prior to use. The reaction was monitored by chromatographic analysis of the gas phase.

Hydrolysis. Hydrolysis was performed under strict exclusion of air, using standard break-seal glass apparatus. Water (vapor pressure) was degassed prior to use. The reaction was monitored by chromatographic analysis of the gas phase.

Thermal Stability of 1. (a) In a Batch Reactor. The sample was loaded under argon into a glass reactor. Argon was removed, and the sample was heated from room temperature to 150 or 250 °C in 2 h. The sample was then heated for 21 h. The reaction was monitored by chromatographic analysis of the gas phase and IR and ^{1}H MAS and ^{13}C CP-MAS NMR spectroscopy.

(b) In a Tubular Continuous Reactor. The sample was loaded under argon into a continuous tubular reactor. The sample was heated at a rate of 50 °C h^{-1} from room temperature to 475 °C. The temperature was carefully recorded as a function of time, and the composition of evolved gas was determined online by gaseous chromatography.

Acknowledgment. We thank Daravong Soulivong for tubular continuous reactor experiments, François Bayard for molecular modeling, Anne Baudouin for 2D NMR spectroscopy, and Céline Dablemont for discussions. We also thank Steven Fiddy, scientist at beam line 7.1, for his help during the recording of the EXAFS data at the SRS of the CCLRC, in Daresbury, U.K. (Project No. 44204). We are grateful to Region Rhône Alpes for financial support (G.T.) and to the Society CEZUS for the samples of HfCl$_4$.

Supporting Information Available: Tables and figures giving a comparison of the analytical data of the grafting of M(CH$_2$*t*Bu)$_4$ (M = Hf, Zr) with SiO$_{2-(800)}$ and NMR, IR, EXAFS spectra and data for (≡SiO)Zr(CH$_2$*t*Bu)$_3$. This material is available free of charge via the Internet at http://pubs.acs.org.

OM060178F

(55) Society, I. X. http://ixs.iit.edu/subcommittee_reports/sc/, 2000.